# Effect of waviness and roughness on cylinder liner friction

Eduardo Tomanik [a,*], Mohamed El Mansori [b], Roberto Souza [a], Francisco Profito [a]

[a] Surface Phenomena Laboratory (LFS), Polytechnic School of University of Sao Paulo, Av. Prof. Mello Moraes, 2231, 05508-030 Sao Paulo, SP, Brazil
[b] ENSAM, MSMP-EA7350, 2 cours des Arts et Métiers, 13617, Aix-en-Provence, France

*Keywords:*
Topography
Waviness
Piston rings
Friction

A B S T R A C T

The tribological performance of piston ring-cylinder bore was investigated through deterministic mixed-lubrication modeling. Bore topographies measured from regular honed Gray Cast Iron (GCI) to "Mirror-Like" coated bore surfaces were used in the investigation. In contrast with typical honed GCI bores composed of relatively well-distributed peaks and valleys, coated bores are composed of a much smoother plateau and localized deep pores. Simulation results indicated that coated bore surfaces generate significantly higher hydrodynamic pressure and lower asperity contacts when compared with regular GCI topographies. The influence of roughness filtering and the associated cut-offs values were also considered in the analysis, showing that the choice of cut-off affects both the predicted hydrodynamic and asperity contact pressures. Furthermore, the simulation results also revealed that most of the fluid pressure was generated by the honing grooves rather than by the localized pores present on coated bore surfaces.

## 1. Introduction

Optimization of surface topography is one of the main paths to improve tribological performance of internal combustion engines (ICEs). Although smoother surfaces are usually associated with low friction and wear, the presence of a controlled amount of roughness on the contact surfaces is in general necessary to prevent adhesion, work as lubricant micro-reservoirs and debris trap, as well as allow contact shape adjustments. For combustion engines, special attention has been given to the finish of cylinder bores. Being the piston system responsible for approximately 50% of the total engine friction losses [1,2], improvements on the cylinder bore surface may lead to significant reduction of fuel consumption and $CO_2$ emissions. For decades, the engine cylinder bores were made of honed Gray Cast Iron (GCI) and honing specification was improved by experience with relative little theoretical basis [3–6]. More recently, use of computer simulation techniques [7–12] allowed a more scientific-based approach to understanding the complex, multi-physical phenomena taken place on piston ring – cylinder bore interactions, thus providing more insights during the design process of cylinder bore topographies.

From the industry side, the introduction of thermal spray coated bores (designated as "CB" throughout this article) has also brought new opportunities for improving the engines' tribological performance in terms of both surface material and the topographic features (e.g. roughness patterns, textures etc.) [13,14]. In contrast to regular GCI bores, coated bores currently in production are significantly smoother and, instead of having a relative regular rough honed surface with plateaus and valleys given by the honing grooves, coated bore surfaces are characterized by (very) smooth plateau regions with localized pores. A special type of such coated bore surfaces, called "Mirror-Like" [15,16], is drastically smoother than the typical GCI bore still in production. Table 1 compares some roughness parameters between GCI and coated bore "Mirror-Like" surfaces of SI engines cylinder bores currently in production; notice that most roughness parameters are 5–10 times smaller for the coated bore.

The smoother coated bore surfaces lead to thinner lubricant film thickness that generates significant higher hydrodynamic pressure and lower asperity interactions, which in turn promotes potential friction reduction under mixed lubrication conditions. Additionally, as new pores are continuously being exposed due to wear, the surface never become completely polished by wear as usual in GCI bores, especially on the engine's reversal Top Dead Center (TDC). On the other hand, the coated bores bring also new challenges for design production and control. For instance, GCI engine blocks and liners have usually their roughness measured by profilometer. Furthermore, typical GCI topographies, although composed of peak, plateaus and honing valleys is somehow homogenous "well-behaved". Relatively few roughness measurements are suitable to capture and control important functional features of the bore surfaces. Localized higher peaks and surface small

* Corresponding author.
*E-mail address:* eduardo.tomanik@usp.br (E. Tomanik).

**Table 1**
Examples of cylinder bore surfaces currently used in modern passenger cars.

| | GCI "slide honing" | Coated bore "Mirror-Like" |
|---|---|---|
| | 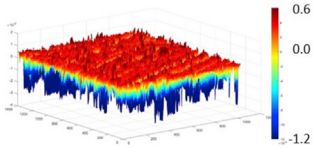 | 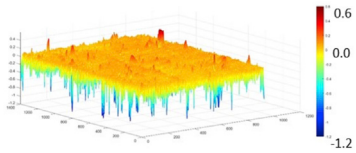 |
| Roughness Parameter | | |
| Sa [μm] | 0.40 | 0.05 |
| Spk [μm] | 0.18 | 0.02 |
| Sk [μm] | 0.42 | 0.06 |
| Svk [μm] | 1.65 | 0.18 |
| Vmp x $10^{-2}$ [$\mu m^3/\mu m^2$] | 8.9 | 2.1 |
| Vmc x $10^{-2}$ [$\mu m^3/\mu m^2$] | 36 | 4.1 |
| Hydro pressure[a] [MPa] | 0.3 @ 0.27 μm | 94.4 @ 0.06 μm |
| Asperity pressure[a] [MPa] | 1.4 @ 0.27 μm | 0.2 @ 0.06 μm |

[a] Calculated with the deterministic simulation described in the present contribution.

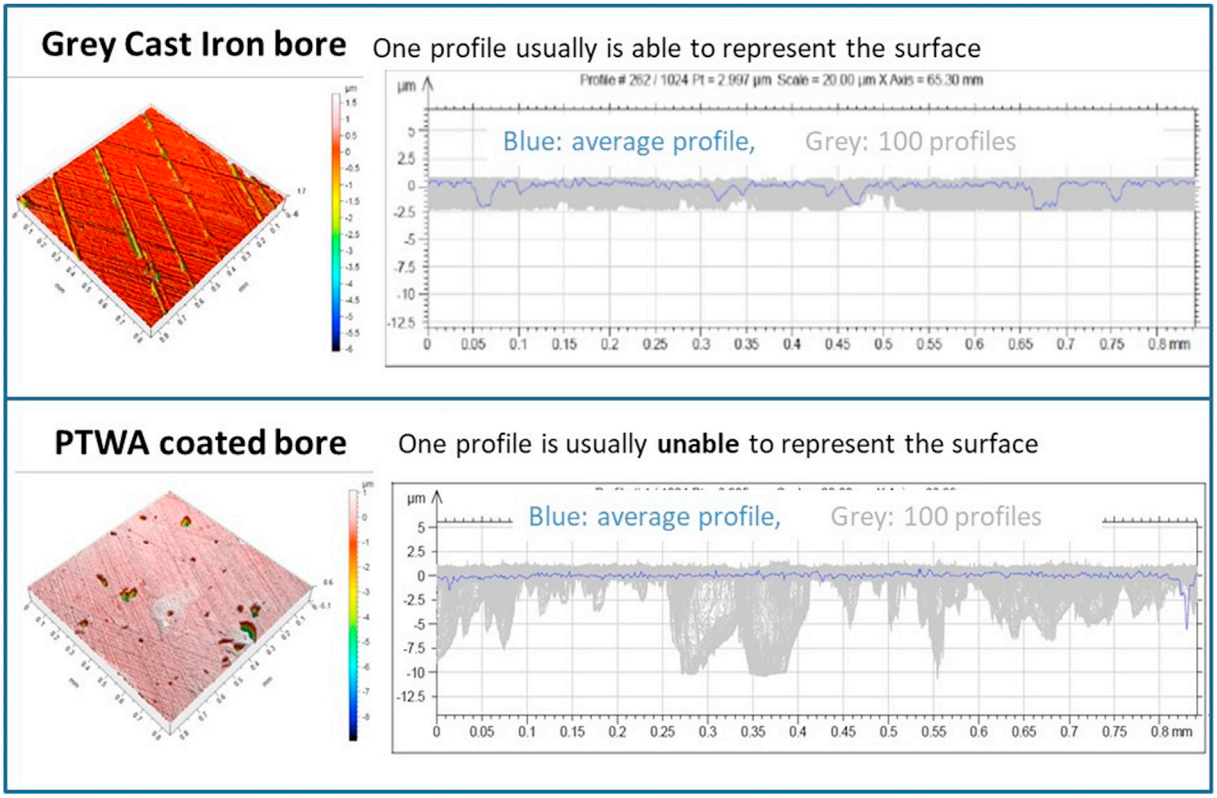


**Fig. 1.** Roughness profiles extracted from 3D roughness measurements of regular GCI and a coated bore cylinder surfaces.

"defects" are in general removed during engine break-in. Smoother coated bores have a less homogenous topography, most of the surface is an almost flat smooth plateau with localized pores. In case of improper thermal spray, some oxidized or unmelted hard protuberances may exist. Fig. 1 compares non-contact optical topography measurements (800 × 800 μm size) of a GCI and a coated bore cylinder surface. For each measured surface, 100 equally spaced roughness profiles (in gray) were extracted and the average profile (in blue) was calculated. While the average profile was able to "represent" the main surface features for the GCI bore (peaks and valley are of the same magnitude of the population), for the coated bore most of the extracted profiles miss the deep pores. The selected coated bore surface illustrated in Fig. 1 has also a protuberance (the white region closer to the center) that would escape from most of the profile measurements. As a consequence of the aforementioned issues, non-contact optical measurement techniques are becoming usual during the development and analysis of engine cylinder bores [17].

## 2. Effect of the waviness filtering and cut-off selection on the rough contact interactions

Fig. 2 shows a profile extracted from a GCI bore surface after waviness filtering with 800, 250 and 80 μm cut-offs. According to ISO 4288, the 800 μm cut-off should be used, since Ra is between 0.10 and 2.0 μm. The unfiltered waviness is almost identical to the filtered one obtained with cut-off 800 μm and the former is not showed here for simplicity. With successive smaller cut-offs, the reference line (red lines in the plots on the left of Fig. 2) better follows the original unfiltered profile. The plots in the center of Fig. 2 show a zoom in of the interval x = 700–1000 μm along the profile length, highlighting the peak regions located around x = 820 μm

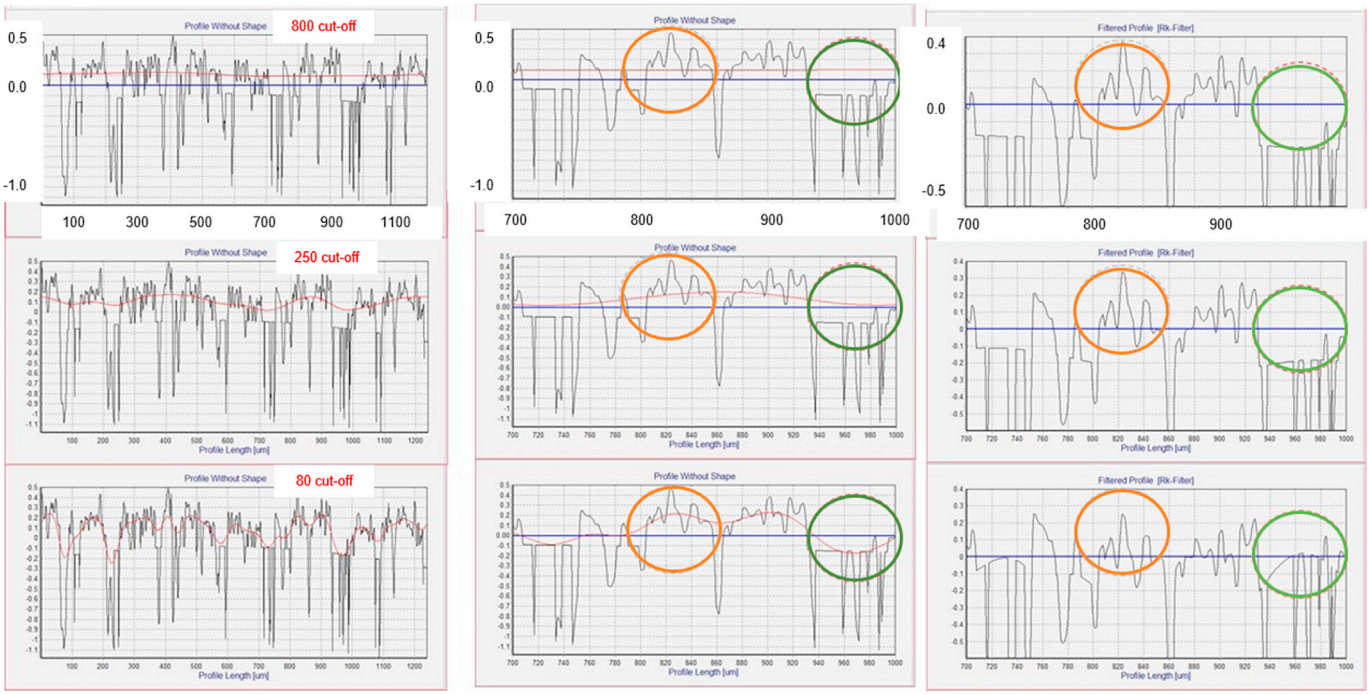


**Fig. 2.** Cylinder bore roughness profiles obtained from different cut-offs.
Left: Form filtered profile. Center: idem, zoom at x: 700–1000 Right: Filtered Roughness.
Blue line: Mean line. Red line: waviness. From top to bottom: 800, 250 and 80 μm cut-offs. (For interpretation of the references to color in this figure legend, the reader is referred to the Web version of this article.)

and a valley region at x = 970 μm. The plots on the right of Fig. 2 illustrate an important effect observed at the highlighted regions, in which shorter cut-offs tend to locally "lower" the peaks and "raise" the valleys. As expected, 80 μm cut-off generated a flatter profile than the 800 μm one, since the shorter cut-off allowed the mean line to follow closely the profile waviness. Overall, although the cut-off choice had

**Table 2**
SEM photos, topographies and typical roughness parameters of the cylinder bores surfaces investigated in the present work.

| | SEM photo | CCI topography | Roughness [μm] | |
|---|---|---|---|---|
| | | | 'W+R' Waviness + Roughness | R250 |
| GCI | 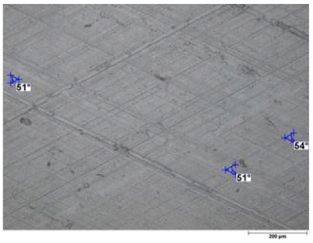 | 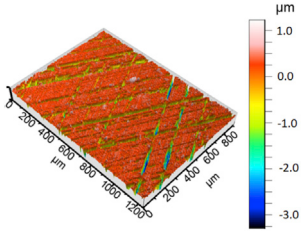 | Sa: 0.43<br>Swt: 0.58<br>Spk: 0.19<br>Sk: 0.50<br>Svk: 1.64<br>Swt/Sa: 1.3 | 0.42<br>0.61<br>0.18<br>0.42<br>1.60<br>1.5 |
| MLJ | 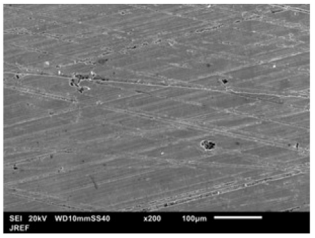 | 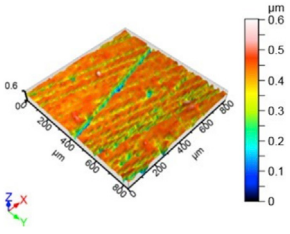 | Sa: 0.06<br>Swt: 1.09<br>Spk: 0.05<br>Sk: 0.10<br>Svk: 0.23<br>Swt/Sa: 16 | 0.06<br>0.60<br>0.04<br>0.04<br>0.22<br>10 |
| MLN | 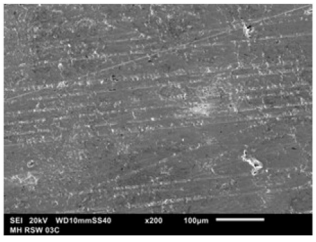 | 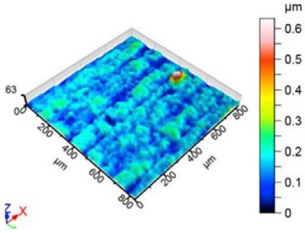 | Sa: 0.05<br>Swt: 0.72<br>Spk: 0.05<br>Sk: 0.16<br>Svk: 0.12<br>Swt/Sa: 14 | 0.04<br>0.22<br>0.04<br>0.09<br>0.11<br>6 |

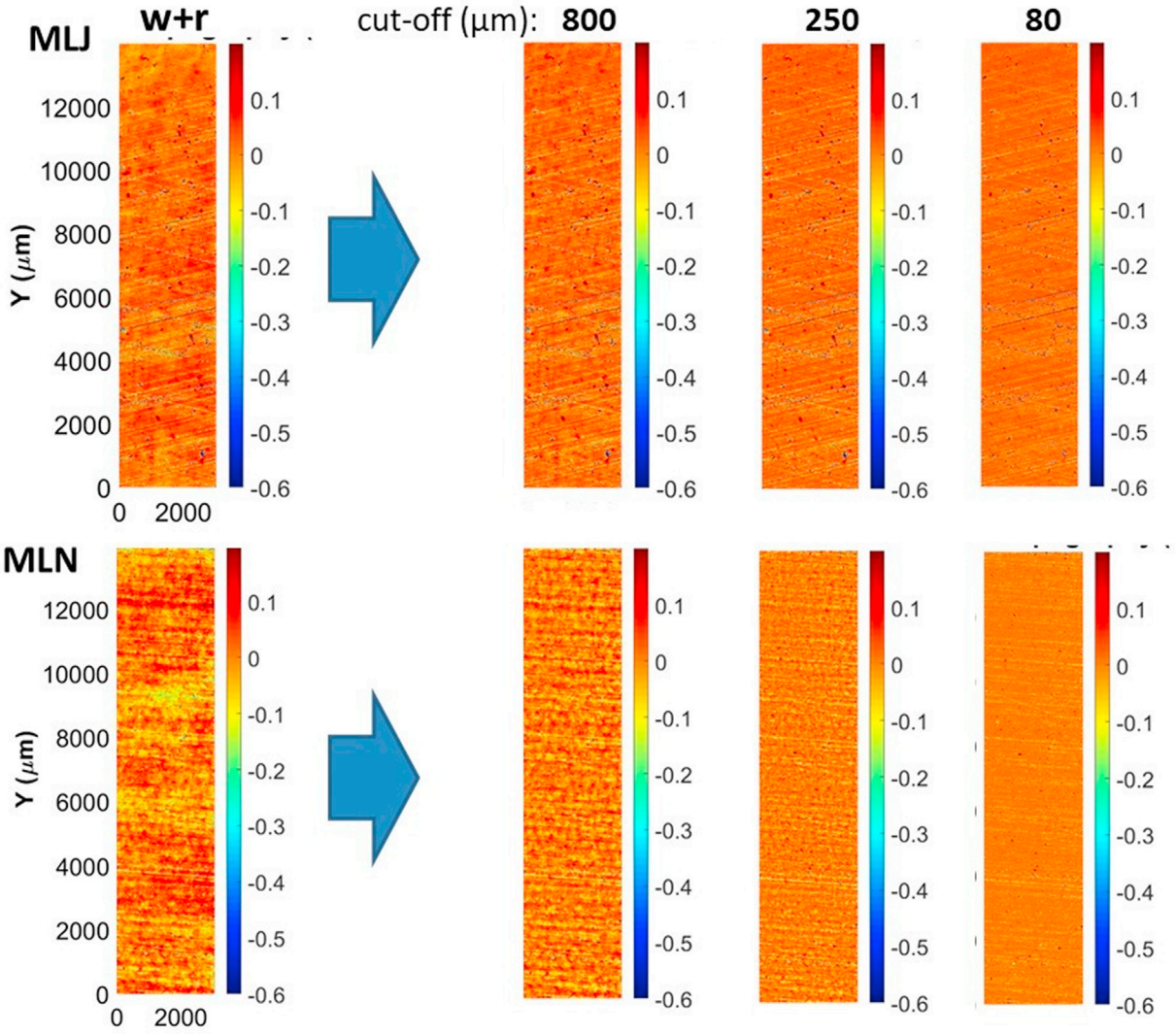


**Fig. 3.** Topographies of the coated bore surfaces investigated in the present work: MLJ surface (top) and MLN (bottom). From left to right: Primary surface (only form removed, 'W+R') and roughness surfaces after waviness filtered with 800, 250 and 80 μm cut-offs.

little effect on the roughness parameters (e.g. Sk = 0.06 μm, 0.06 μm, 0.04 μm, respectively, for cut-offs of 800, 250, 80 μm; see more details in Annex 1), it locally affected the peaks and valleys of the filtered surface, which in turn may influence deterministic calculated hydrodynamic pressure and asperity contacts under mixed lubrication conditions.

It is worth noticing that under real contact conditions, a sliding surface encounters the actual surface geometry including both the form and waviness components, and not the filtered profile/surface. At the same time, how close a sliding body will follow the actual, unfiltered profile/surface depends on the contact length. A wider contact length tends to interact with all the form and waviness deviations of the surface, while a shorter one may be able to follow the form deviations and "contact" only the waviness and roughness. Similarly, an even shorter contact length may interact only with the roughness peaks. The tendency of contact of a sliding body against the different surface components (form, waviness and roughness) is also dependent on the surfaces separation (or oil film thickness in case of lubricated systems). The smaller the separation, more a wider contact surface length will be sensitive to the waviness and roughness deviations.

## 3. Coated bore surface investigated cases

Two SI engine coated bore surfaces were selected for the investigations of the present contribution. The first one (denoted as MLJ) is a "Mirror-Like" type used in a Japanese car, which is currently considered one of the benchmarks in terms of bore surface and low friction. The second coated bore (designated as MLN) is an European one still in development, whose both coating and honing process were still under optimization when the samples were obtained, but the target honing is also to be "Mirror-Like". The two cases also differ in terms of surface preparation before coating to improve coating adherence, coating powder composition, and thermal spray method, but only the topographic features of the surfaces will be considered in the current investigation. MLJ samples were cut from an original engine block in production and MLN ones from a Gray Cast Iron tube used during the development of the coating and honing. Table 2 shows typical SEM photos, surface roughness and some selected roughness parameters of the investigated topographies (see complete table in Appendix 1). Notice that most of the roughness parameters are 5–10 times lower for the two coated bores in comparison with conventional GCI surfaces. The exception is the waviness height that is of the same magnitude order. Hence, the ratio Swt/Sa changed from about 1.5 for the GCI to approximately 15 (before waviness filtering) and 10-6 (after waviness filtering with cut-off 250 μm) for the coated bores. In a previous work [18], the authors discussed how the cut-off filtering choice affect the asperity contact for GCI surfaces. One can expect that the effect of waviness might be more

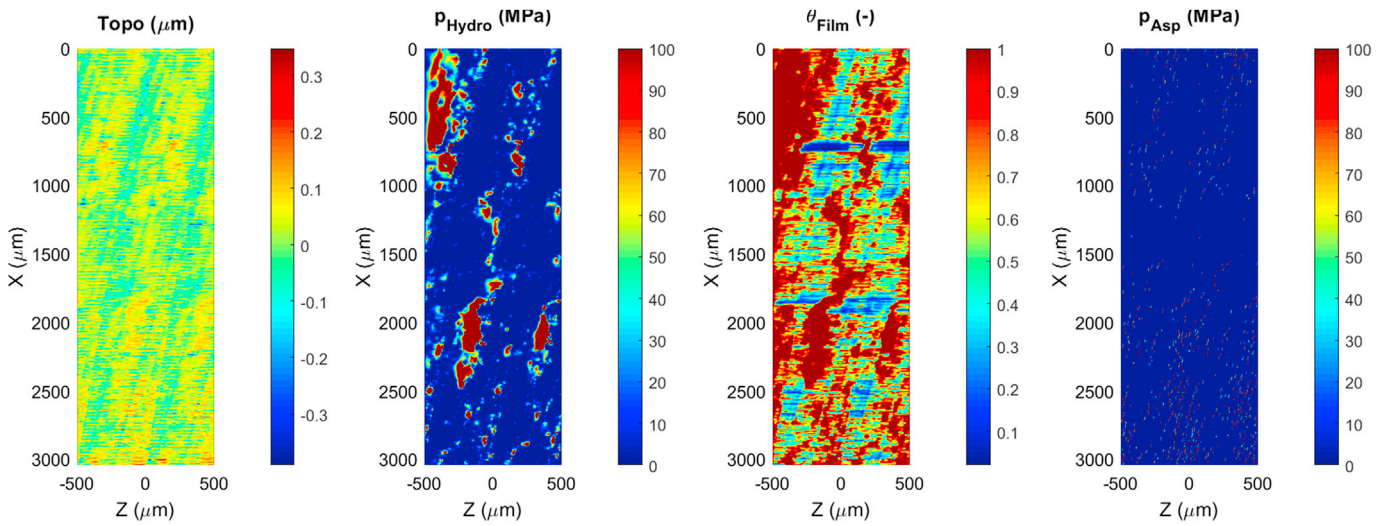


**Fig. 4.** Surface heights, hydrodynamic pressure, lubricant film ratio and asperity contact pressure for MLN slice 3, "W+R", $\Lambda = 1.5$. For better visualization, the maximum value on the color scale on the pressure fields was fixed at 100 MPa. The reader is referred to the web version of this article for the MATLAB original plots. (For interpretation of the references to color in this figure legend, the reader is referred to the Web version of this article.)

significant on the smoother coated bore surfaces, especially because of the consequent lower oil film thickness promoted by smoother surfaces. Furthermore, the lower oil film thickness associated with the low viscosity oils nowadays in use in modern engines probably intensify such effect.

## 4. Effect of waviness filtering

The surfaces measurements were conducted in a non-contact interferometer Taylor-Hobson CCI (Coherence Correlation Interferometry) using 10× lens magnification with $1024 \times 1024$ pixels of resolution. Individual $0.8 \times 0.8$ mm measured areas were automatically stitched to generate a $14 \times 3$ mm topography, which was then analyzed using the TalyMap software supplied by the equipment manufacturer. Initially, the cylindrical form of the surfaces was removed, followed by the application of a "denoising" filter (also called S-Filter) aimed at removing short-scale components (the so-called "microroughness") usually associated with instrument or environmental noise [21,22]; Robust Gaussian filter with 4x pixel size cut-off was adopted for microroughness removal. The reason for applying a "denoising" filter was to eliminate unrealistic geometrical artifacts that could disturb the convergence of the numerical solution. Subsequently, Robust Gaussian filter with 80, 250 and 800 cut-offs was used to obtain the correspondent roughness surfaces and then the roughness parameters were calculated. In addition to the roughness parameters, the x,y,z data of the surfaces before and after waviness filtered were exported as input files for the computational simulations described in Section 5.

Fig. 3 illustrates the waviness filtering effect. Despite the slightly higher Swt, the presence of waviness valleys and peaks is less visually evident on the MLJ surface, and the roughness height distribution is more homogenous. On the other hand, lower regions around $x = 1500$, 6000 and 9000 μm, as well as higher regions around $x = 3000$, 7000 and 12000 μm, are visible on the MLN surface. As can be seen in Fig. 3, after waviness filtering with 250 μm cut-off, such lower and higher regions were eliminated from the MLN surface, i.e. MLN surface became flatter and smoother with smaller roughness height distribution.

## 5. Deterministic simulation of the mixed-lubrication regime

The study of mixed-lubrication using 3D measured topographies and deterministic computer modeling is becoming widespread in both academia and industry. However, hydrodynamic and asperity contact pressures depend on all scale components of the surface topography and not only on the filtered roughness commonly provided by many measuring procedures. Characterization of areal surface topographies is still a challenge, since the use of 3D filtering techniques for separating the different surface components (i.e. form, waviness and roughness), as well as the definition of proper measurement parameters, have not been well-established in the literature. Besides, due to the small size of 3D measurement regions, standard procedures designated to 2D profiles are in general not applicable for 3D topographies.

The deterministic mixed-lubrication modeling described in Refs. [11,12,18] was used to assess the influence of the waviness filter and the associated cut-off values on the hydrodynamic pressure generation and asperity interactions for the coated bore surfaces investigated in the present contribution. The contact between the measured bore topographies against a parallel, flat and rigid sliding plane is considered. In this case, since the contact is assumed to be between two parallel and flat surfaces, the topographic irregularities (waviness and roughness) along with the inter-asperity cavitation are the solely responsible for the generation of hydrodynamic pressures. For different surfaces separations, the Reynolds equation with p-θ Elrod-Adams mass conserving cavitation model is solved simultaneously with a Hertzian-based elastic-perfectly plastic model for rough contact pressures calculation. At every asperity contact spot, it is assumed solely the occurrence of contact pressures with no hydrodynamic effects (boundary contact); a threshold value of 1 nm is adopted as the minimum allowed film thickness in order to avoid singularities in the solution of Reynolds equation.

The following input data was used in the simulations:

- Sliding velocity: 3 m/s
- Dynamic viscosity: 0.01 Pa s
- Lubricant density: 850 kg/m$^3$
- Combined Young Modulus: $1.2 \times 10^{11}$ Pa

Simulations were carried out for the investigated coated bores (MLJ and MLN) considering 4 cases: (a) surfaces with only form removal (hereafter designated as 'W+R'), i.e. the primary surfaces including both the waviness roughness components; waviness filtered surfaces with (b) 800 μm, (c) 250 μm and (d) 80 μm cut-off. A longer than usual sliding surface length of 1 mm was used in the simulation in order to evaluate the influence of wider top piston-rings, especially after wear, or the relatively long piston skirt.

The deterministic calculations were truncated at $\Lambda = 1.5$, where $\Lambda$ is

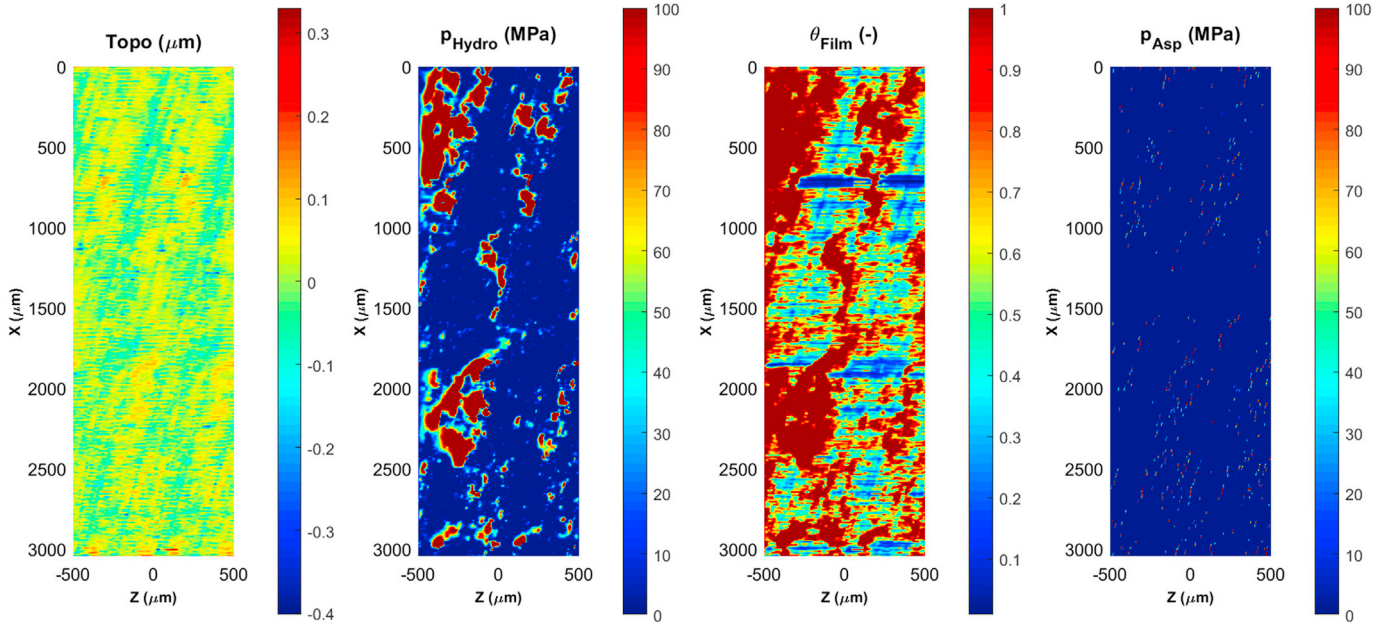


**Fig. 5.** Surface heights, hydrodynamic pressure, lubricant film ratio and asperity contact pressure for MLN slice 3, waviness filtered 800 μm cut-off, $\Lambda = 1.5$.

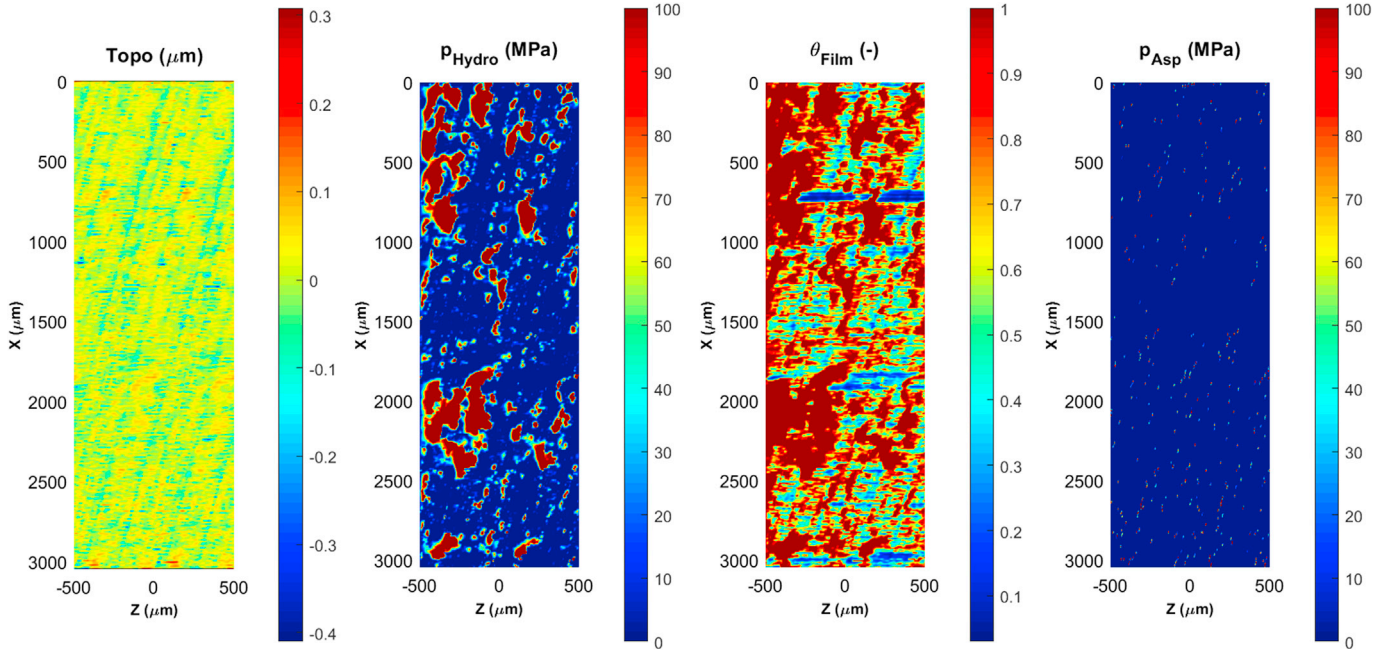


**Fig. 6.** Surface heights, hydrodynamic pressure, lubricant film ratio and asperity contact pressure for MLN slice 3, waviness filtered 250 μm cut-off, $\Lambda = 1.5$.

the dimensionless film thickness defined as the ratio between the surfaces separation and the combined roughness, i.e. $\Lambda = H_m/Sq$. However, it is important to notice that even considering such truncation, the predicted film thickness associated with $\Lambda = 1.5$ was only 0.15 μm for MLJ and 0.09 μm for the MLN, which in turn tend to stress the assumptions of the adopted mathematical models, especially regarding the lubricant rheological behaviour under high shear rate conditions as those promoted by such thin lubricant film thickness. In general, the MLN bore surface presented considerably higher hydrodynamic and asperity pressures. This tendency might be related to the fact that the actual film thickness for the MLN surface is approximately 40% smaller when compared with the MLJ one, hence contributing to the generation of higher hydrodynamic pressures and more asperity interactions.

Figs. 4–7 illustrate the MLN bore slice 3 (y = 2000–3000 μm in Fig. 3) with dimensionless surface separation of $\Lambda = 1.5$ and the calculated hydrodynamic pressure and lubricant filling ratio (cavitation) fields for the 4 analyzed cases ("W+R", 800, 250 and 80 μm cut-off). According to the figures, most of the hydrodynamic pressures were generated by the honing grooves rather than by the localized pores present on coated bore surfaces. Particularly for the slice 3 in analysis, smaller cut-off values lead to flatter surfaces, which in turn promoted an increase in the lubricant filling ratio and hydrodynamic pressure. The asperity contact pressure reduced with the surface flattening.

According to Figs. 4–7, it is possible to identify some interrelated aspects that significantly influenced the generation of hydrodynamic and asperity contact pressures. The first aspect is associated with the number

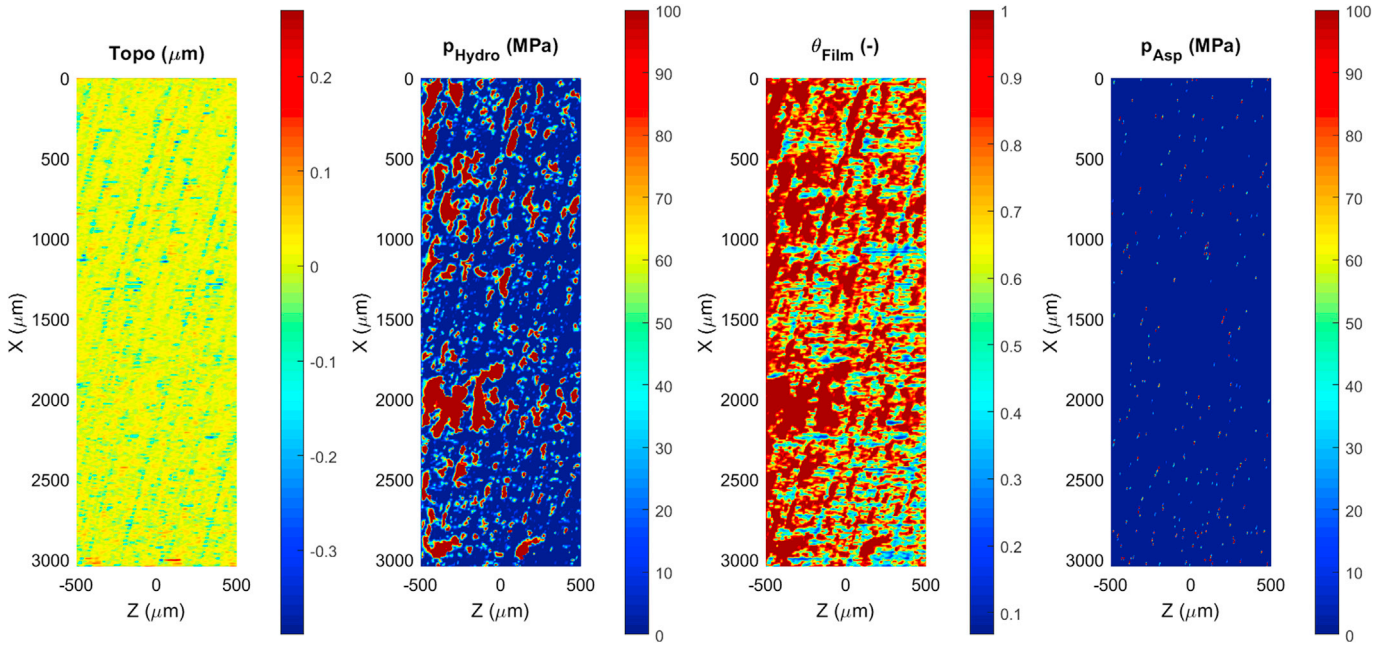


**Fig. 7.** Surface heights, hydrodynamic pressure, lubricant film ratio and asperity contact pressure for MLN slice 3, waviness filtered 80 μm cut-off, $\Lambda = 1.5$.

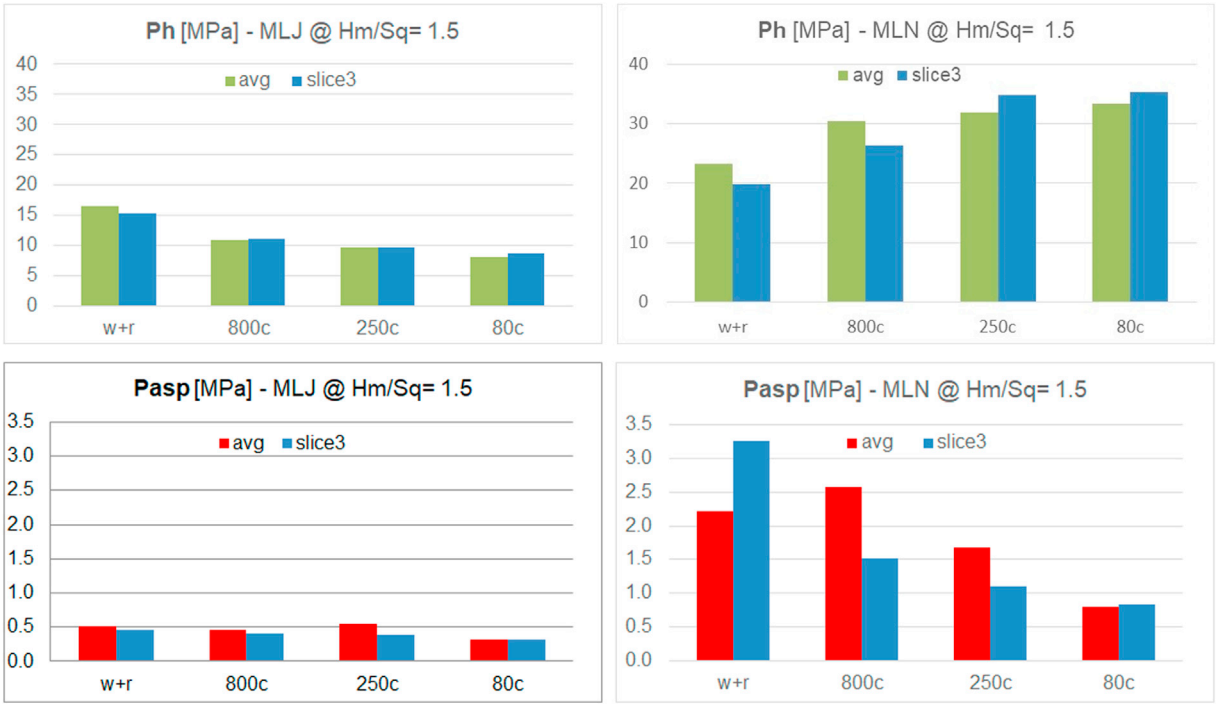


**Fig. 8.** Average hydrodynamic and asperity contact pressures for the entire stitched surface and for slice 3. $\Lambda = 1.5$.

of asperities in contact, which is directly dependent on the roughness of the plateau regions along with the cut-off value adopted for the waviness filtering. As can be seen in the surface plots of asperity pressure in Figs. 4–7, and reminding that in all cases the dimensionless surfaces separation is retained constant ($\Lambda = 1.5$), the amount of contact spots decreases as the surface is flattened by progressively shorter waviness filtering cut-offs. Correspondently, such reduction in interaction between the surfaces' asperities is followed by a gradual increase in the hydrodynamic pressure distribution throughout the contact interface (see the surface plots of hydrodynamic pressure in Figs. 4–7). This effect may be explained by the ease with which the lubricant flows through the rough interface when fewer asperities are in contact, thus contributing to fluid pressure build-up. In fact, when more asperities are in contact, the formed local junctions tend to disrupt the full development of the lubricant flow, which inevitably affects the overall lubrication mechanism. The combined effect of plateau roughness and surface flattening due to the use of different waviness filtering cut-offs described above and its influence on raising the hydrodynamic pressure and lowering the asperity contact pressure can also be observed in Fig. 8 for the MLN case.

Fig. 8 shows the average hydrodynamic and asperity contact pressures for the both the entire stitched surface and for slice 3 (both cases for $\Lambda = 1.5$). The MLJ surface showed smaller average hydrodynamic and

**Table 3**
Surface Roughness parameters.

| | | GCI | | MLJ | | | | MLN | | | |
|---|---|---|---|---|---|---|---|---|---|---|---|
| | | 'W+R' | 250 | 'W+R' | 800 | 250 | 80 | 'W+R' | 800 | 250 | 80 |
| Sa | µm | 0.43 | 0.42 | 0.06 | 0.06 | 0.06 | 0.10 | 0.05 | 0.04 | 0.04 | 0.05 |
| Sq | µm | 0.61 | 0.61 | 0.10 | 0.10 | 0.09 | 0.10 | 0.07 | 0.06 | 0.06 | 0.06 |
| Spq | µm | – | – | 0.04 | 0.02 | 0.02 | 0.02 | 0.06 | 0.04 | 0.04 | 0.04 |
| Swt | µm | 0.58 | 0.61 | 0.96 | 0.10 | 0.60 | 1.10 | 0.72 | 0.04 | 0.22 | 0.73 |
| Spk | µm | 0.19 | 0.18 | 0.05 | 0.04 | 0.04 | 0.04 | 0.05 | 0.04 | 0.04 | 0.04 |
| Sk | µm | 0.50 | 0.42 | 0.10 | 0.06 | 0.06 | 0.04 | 0.16 | 0.09 | 0.09 | 0.10 |
| Svk | µm | 1.64 | 1.60 | 0.23 | 0.21 | 0.22 | 0.20 | 0.12 | 0.11 | 0.11 | 0.11 |
| Smr1 | % | 6.6 | 7.4 | 7.8 | 7.9 | 7.1 | 8.6 | 8.4 | 7.4 | 7.4 | 7.9 |
| Smr2 | % | 74.7 | 73.9 | 79.1 | 75.2 | 74.9 | 74 | 87.6 | 85.4 | 85.4 | 83.6 |
| Vmp E-3 | $\mu m^3/\mu m^2$ | 9.2 | 8.9 | 2.3 | 2.2 | 2.1 | 1.7 | 2.8 | 1.9 | 1.9 | 2.3 |
| Vmc E-2 | $\mu m^3/\mu m^2$ | 37.3 | 36.2 | 4.7 | 4.5 | 4.1 | 3.4 | 5.9 | 3.8 | 3.8 | 4.9 |
| Vvc E-2 | $\mu m^3/\mu m^2$ | 28.4 | 25.8 | 4.8 | 4 | 3.5 | 2.8 | 7.5 | 4.7 | 4.7 | 6.1 |

asperity pressures than the MLN one, and the calculated pressures were relatively little affected by the waviness filtering. On the other hand, the MLN surface showed a trend of increase in the hydrodynamic pressure and decrease in the asperity pressure with use of smaller cut-off values.

## 6. Conclusions

With the ever-increasing use of smoother cylinder surfaces of internal combustion engines, like "Mirror-Like" coated bore surfaces, more attention is needed for the separation of the waviness and roughness components of areal surface topographies, especially when deterministic mixed-lubrication simulations are considered. The irregular distribution of very smooth plateaus and localized deep pores demand more use of surface measurements rather than conventional profilometer techniques. The usual small 3D measurement sizes obligate the adoption of small cut-off lengths during the surface filtering process, which generally eliminates important components of the existent surface waviness that might affect locally the mechanisms of mixed-lubrication.

In the present work, two "Mirror-Like" coated bores, one in production (MLJ) and other still under development (MLN), were initially characterized using non-contact interferometer measurements and waviness filtered with different cut-off lengths. Afterwards, the obtained surface roughness were used as input for computational simulations of the mixed-lubrication regime based on deterministic models. The simulation results indicated the tendency of hydrodynamic pressure rise at the convergent portion of the honing grooves, especially on the smooth plateaus regions after the grooves. The localized deep pores were too few and deep to promote a substantial generation of hydrodynamic pressure. Overall, the calculated hydrodynamic and asperity pressures varied depending on the selected cut-off length. For the MLN surface, the effect of cut-off was more significant, increasing the hydrodynamic pressure and reducing the asperity contact interactions for shorter cut-off values. On the other hand, for the MLJ surface, the fluid pressure decreased whereas the asperity contact pressure remained almost unchanged for shorter cut-offs. Furthermore, it was identified two interrelated aspects that influence the occurrence of fluid pressure build-up and asperity contact under mixed-lubrication between parallel and flat rough surfaces. As the surface is flattened due to the use of shorter cut-off values, the hydrodynamic pressure tends to rise while the asperity interactions decrease. However, it is worth highlighting that the Reynolds equation based model used in this work is not suitable to properly reproduce the lubricant flow within pores or other very deep topographic features (see more in-depth discussions about the effect of dimples on lubrication in Refs. [19,20]).

Another aspect not explored in this study and that should be relaxed in future studies, is that in most of the current simulations the ring is assumed smooth. Such assumption is no longer valid for the "Mirror-Like" coated bores since in this case the bore is often smoother than the ring running face.


## Acknowledgements

The work was supported by the Sao Paulo state funding agency FAPESP, on the project "Future tribological challenges on Flex-Fuel engines", grant 2009/54891-8.

A part of the samples was kindly supplied by Nagel Maschinen-und Werkzeugfabrik GmbH, Nürtingen/German.


## Appendix A. Supplementary data

Supplementary data related to this article can be found at https://doi.org/10.1016/j.triboint.2018.01.012.

## Annex I. Surface roughness parameters of MLJ and MLN coated bores

Table 3 shows the surface roughness of a typical GCI and the two coated bores of the current investigation. While for the GCI case, the height waviness (Swt) is of same order than the average roughness (Sa) in the unfiltered measurement ('W+R'), for the mirror like coated bores, Swt is around 10 times higher than Sa. For the coated bores, notice also as shorter cut-offs significantly increase the waviness height.

## References


[1] Holmberg K, Andesson P, Erdemir A. Global Energy consumption due to friction in passenger cars. Tribol Int 2012;47:221–34.
[2] Schommers J, et al. MTZ 07-08/2013. Minimizing friction in combustion engines, vol. 74; 2013.
[3] Robota A, Zwein F. MTZ 60. Influence of cylinder bore topography on the oil consumption and particulate emissions of a DI TCI diesel engine, vol. 4; 1999.
[4] Sato O, et al. Improvement of piston lubrication in a diesel engine by means of cylinder surface roughness. SAE paper 2004-01-0604. 2004.
[5] Tomanik E. Friction and wear bench tests of different engine liner surface finishes. Tribol Int 2008;41:1032–8.
[6] Anderberg C, Dimkovksi Z, Rosen B. Liner surface improvements for low friction ring packs. Surf Topogr: Metrol Prop 2014;2, 014009.
[7] Chen H, Li Y, Tian T. A novel approach to model the lubrication and friction between the twin-land oil control ring and liner with consideration of micro structure of the liner surface finish in internal combustion engines. SAE paper 2008-01-1613. 2008.
[8] Mezgahni S, et al. Energy efficiency optimization of engine by frictional reduction of functional surfaces of cylinder ring-pack system. Tribol Int 2013;59:240–7.
[9] Mezghani S, et al. Mutual influence of cross hatch angle and superficial roughness of honed surfaces on friction in ring-pack tribo-system. Tribol Int 2013;66:54–9.
[10] Spencer A, et al. An experimental and numerical investigation of frictional losses and film thickness for four-cylinder liner variants for a heavy duty diesel engine. Proc IME J J Eng Tribol 2013;227(12).
[11] Profito F, Tomanik E, Zachariadis D. Effect of cylinder liner wear on the mixed lubrication regime of TLOCRs. Tribol Int 2016;93:723–32.
[12] Profito F, et al. Transient experimental and modelling studies of laser-textured micro-grooved surfaces with a focus on piston-ring cylinder liner contacts. Tribol Int 2016;113:125–36.
[13] Hahn M. The impact of microstructural alterations at spray coated cylinder running surfaces of diesel engines – findings from motor and laboratory benchmark tests. Wear 2011;271:2599–609.

[14] Morawitz U, Mehring J, Schram L. Benefits of thermal spray coatings in internal combustion engines, with specific view on friction reduction and thermal management. SAE paper 2013-01-0292. 2013.
[15] Schommers J, et al. Minimizing friction in combustion engines, vol. 74. MTZ; 2013. p. 28–35.
[16] Sui T, et al. Development of friction reduction technology for the new 1.2L 3 cyl. Gasoline engine. JSAE Paper No. 20115586. 2011.
[17] Pehnelt S, et al. Assessment of 3D parameters for the characterisation of cylinder treads, vol. 74. MTZ; 2013. p. 44–8.
[18] Dimkovski Z, Tomanik E, Profito F. Influence of measurement and filtering type on friction predictions between cylinder liner and oil control ring. Tribol Int 2016;100:1–7.
[19] Profito F, et al. Transient experimental and modelling studies of laser-textured microgrooved surfaces with a focus on piston-ring cylinder liner contacts. Tribol Int 2017;113:125–36.
[20] Vladescu S, et al. Looking into a laser textured piston ring-liner contact. Tribol Int 2017;115:140–53.
[21] Leach RK. Fundamental principles of engineering nanometrology. Amsterdam: Elsevier; 2009.
[22] ISO/DIS 25178 part 2. Geometrical product specification (GPS) - surface texture: areal - Part 2: terms, definitions and surface texture parameters. International Organization for Standardization; 2007.

## Nomenclature

*CB:* coated Bore
*GCI:* Gray Cast Iron
$H_m$*:* Minimum Oil Film thickness (surface separation)
*ML::* Mirror-Like
$P_{asp}$*::* Asperity pressure
$P_h$*:* Hydrodynamic Pressure
*Sa:* Average Roughness
*SI:* spark Ignited
*Sq:* Root mean square height
*Swt:* Height of waviness
*Spk:* Reduced peak height
*Sk:* Core roughness height
*Svk:* Reduced Valley depth
*Vmp::* Peak material volume ($p = 10\%$)
*Vmc:* Core material volume ($p = 10\%$; $q = 80\%$)
*Vvc:* Core void volume ($p = 10\%$; $q = 80\%$)
*'W+R':* Primary surface including Waviness and Roughness components
*Λ:* Dimensionless film thickness (surface separation), $\Lambda = H_m/Sq$